HHS Public Access

Author manuscript

Dev Dyn. Author manuscript; available in PMC 2020 November 20.

Published in final edited form as:

Dev Dyn. 2020 June ; 249(6): 765–774. doi:10.1002/dvdy.157.

Mutational analysis of genes with ureteric progenitor cell specific expression in branching morphogenesis of the mouse kidney

Elisabeth A. Rutledge[1], **Andrew P. McMahon**[*,1]

[1]Department of Stem Cell Biology and Regenerative Medicine, Eli and Edythe Broad-CIRM Center for Regenerative Medicine and Stem Cell Research, W.M. Keck School of Medicine of the University of Southern California, CA 90089, USA

Abstract

Background—Ureteric progenitor cells (UPCs) within the branch tips of the arborizing ureteric epithelium of the kidney's developing collecting system establish the shape and cellular organization of the collecting network, and drive the nephrogenic program through their interactions with nephron progenitor cells. In a previous study, expression screening identified a cohort of genes showing UPC-enriched expression including *D17H6S56E-5*, *Hs3st3a1*, *Hs3st3b1*, and *Tmem59l*. Each of these is also enriched in branch tips of assembling airways of the developing lungs. Here, we used Crispr-CAS9 directed gene editing to mutate each of these targets to address their potential role(s) in UPC programs.

Results—Single (*D17H6S56E-5* and *Tmem59l*) and double (*Hs3st3a1* and *Hs3st3b1*) mutants were viable, fertile, and displayed varying frequencies of ureter duplications and no overt lung phenotype. Ureter duplications arise spontaneously through multiple outgrowths of the ureteric bud at the onset of kidney development. *Tmem59l* mutants and *Hs3st3a1*/*Hs3st3b1* compound mutants showed a weakly penetrant, but statistically significant increase in duplicated ureters compared to C57BL6/J and SW wildtype mouse strains.

Conclusions—*Tmem59l* and *Hs3st3a1*/*Hs3st3b1* activities contribute to the regulatory programs restricting ureteric outgrowth in the developing mouse kidney. However, the low penetrance of the observed phenotype precludes detailed analysis of their specific actions.

Keywords

kidney; ureteric progenitor cells; gene knockout; branching morphogenesis; double ureter

INTRODUCTION

Branching morphogenesis is a developmental process that generates a complex arborized epithelial network in a variety of mammalian organ systems, including the kidney and lung.

[*]Corresponding author: Dr. Andrew P. McMahon, Department of Stem Cell Biology and Regenerative Medicine, Eli and Edythe Broad-CIRM Center for Regenerative Medicine and Stem Cell Research, W.M. Keck School of Medicine of the University of Southern California, CA 90089, USA. amcmahon@med.usc.edu.

Declarations of interest: none

[1,2] In the mouse, kidney development initiates at E10.5 with the outgrowth of the ureteric bud (UB) from the nephric duct at the hindlimb region. The UB uses branching morphogenesis to create the collecting duct system which plays a critical role in water, salt and pH balance, and the transport of urine to the ureter for removal from the kidney. The UB consists of two major cell populations: the highly proliferative branch tips made up of ureteric progenitor cells (UPCs) and non-branching stalk regions where differentiated UPC derivatives form.[3] Reciprocal interactions between UPCs and distinct mesenchymal progenitor populations (nephron and interstitial) surrounding the branch tips drives assembly of the mammalian kidney.[4] Molecular analyzes have highlighted shared features of regulatory interactions in branching morphogenesis of the kidney with other organs with prominent branching epithelial programs, notably the lung.[5–7]

In earlier work, we conducted an RNA expression screen comparing the UPC population in ureteric branch tips, with their non-branching cellular derivatives in the ureteric stalk population.[8] In addition to identifying well established branch tip-enriched gene expression for *Wnt11*, *Ret*, *Etv4/5*, and *Sox8/9*, and several other genes, the screen identified and validated branch tip-enriched expression for a large number of genes not previously mapped to the UPC population. Comparative analysis showed 48% of the kidney tip-specific genes identified were also expressed in the embryonic lung tip population, suggesting a potential core branching program. For further investigation, we selected four novel genes (*D17H6S56E-5*, *Hs3st3a1*, *Hs3st3b1*, *Tmem59l*) from this list and generated knockout mouse lines through CRISRP/Cas9 gene editing to determine if these genes are required for normal morphogenesis of kidney and lung.

*D17H6S56E-5 (*alternatively *G7e)* was chosen for analysis given the paucity of information on this gene. First identified in 1996 as a gene within the mouse MHC Class III region[9], *D17H6S56E-5* nucleotide sequence has some homology with murine leukemia virus envelope genes, and its predicted protein structure contains viral envelope motifs.[9] The absence of an obvious ortholog in other mammals suggests a newly acquired mouse gene.

Hs3st3a1 and *Hs3st3b1* are tightly linked genes, encoding closely related type II integral membrane proteins of the heparin sulfate 3-O-sulfotransferase family. These enzymes perform the rare 3-O-sulfation as the final step of heparin sulfate modification within the Golgi apparatus.[10–13] Hs3st3a1 and Hs3st3b1's sulfotransferase domains are highly similar and act on the same disaccharide, suggesting potential redundant functional activities where expression overlaps.[14] Modifications to heparin sulfate allows for biodiversity within these proteoglycans to assist with their numerous specialized functions. Heparin sulfate proteoglycans are known co-receptors for Fgfr2b, which is a key component in kidney and lung branching morphogenesis within Fgf signaling.[15] Both genes are also expressed in the submandibular gland (SMG) endbuds during salivary grand branching morphogenesis[16] where 3-O-heparin sulfate is suggested to stabilize the Fgf10/Fgfr2b complex to promote MAPK signaling and the expansion of the progenitor population within the endbuds.[16] Hence, *Hs3st3a1* and *Hs3st3b1* were selected as potential mediators of cell signaling. Additionally, it has been shown that signaling by glial cell line-derived neurotrophic factor (GDNF), an important regulator of kidney branching, requires the presence of heparan sulfate glycosaminoglycans to induce neuronal axonogenesis.[17,18] Thus, heparan sulfate

modifying enzymes may impact multiple pathways regulating branching morphogenesis of the mammalian kidney.

Tmem59l (transmembrane protein 59-like) is a single-pass type I membrane glycoprotein expressed within the Golgi apparatus that has not been functionally examined in branching morphogenesis. First identified in the human brain as BSMAP (brain-specific membrane-anchored protein), Tmem59l was suggested to have caspase-dependent apoptotic activity and modulate amyloid precursor protein shedding.[19–21] Furthermore, mouse behavioral studies have implicated the downregulation of Tmem59l in reducing depression and anxiety, while increasing memory.[21]

RESULTS

Identification of Four Ureteric Bud Tip-specific Genes

D17H6S56E-5, *Hs3st3a1*, *Hs3st3b1*, and *Tmem59l* where identified in a bulk RNA sequencing screen comparing the ureteric tip population (Wnt11-RFP$^+$/Hoxb7-GFP$^+$) to non-branch tip regions (Hoxb7-GFP$^+$) in the developing ureteric epithelium of the E16.5 mouse kidney [Fig. 1A–C].[8,22,23] All genes show highly enriched expression in UPCs in ureteric branch tips [Fig. 1D]. Whole-mount *in situ* hybridization (WISH) showed *D17H6S56E-5* and *Hs3st3a1* were broadly expressed in the kidney shortly at an early branching stage (E12.5), restricting to the branch tip population by E15.5 [Fig. 1 E, F, I, J]. In contrast, *Hs3st3b1* and *Tmem59l* were tip-restricted from early stages of kidney development [Fig. 1G, H, K, L]. WISH was also performed on mouse embryonic lungs to compare expression patterns between two organs that develop through branching morphogenesis. *D17H6S56E-5* and *Hs3st3a1* were broadly expressed at E12.5, restricting to airway branch tips by E15.5 [Fig. 1M, N, Q, R], *Tmem59l* was tip-specific throughout lung development [Fig. 1P, T] and *Hs3stsb1* was transiently expressed within the lung epithelium at E12.5, but absent from airway epithelium by E15.5 [Fig. 1O, S].

Generation of Knockout Mouse Strains via CRISPR/Cas9 Gene Editing Techniques

To determine the function of D17H6D56E-5, Hs3st3a1, Hs3st3b1, and Tmem59l, knockout mouse strains were generated by CRISPR/Cas9 deletion techniques.

D17H6S56E-5 is located on Chromosome 17 and comprises 3 exons spanning 4,023 base pairs encoding a 596 amino acid sequence with a transmembrane feature at amino acid positions 553–579. CRISPR/Cas9 gene editing removed 1,691 base pairs within exon 2 spanning the transmembrane sequence [Fig. 2A]. The predicted protein product results in a 32 amino acid truncated protein with 13 missense amino acids at the C-terminus from the deletion generated frame shift.

Tmem59l is a 3.5kb gene on Chromosome 8 with 8 exons. Through CRISPR/Cas9 deletion, we removed an 804bp region which includes exon 2 and the N-terminus of exon 3 [Fig. 2B] leading to a new in-frame STOP codon within Exon 3. The resulting allele is predicted to encode a 50 amino acid C-terminal truncated protein product where the final 7 amino acids resulting from the frame shift are missense. The truncated protein would lack the transmembrane sequence encoded by exon 7.

Hs3st3a1 and *Hs3st3b1* are both located on Chromosome 11 on opposite strands within 511 kilobases between their promoter regions suggesting that they are likely co-regulated by similar mechanisms in the kidney where co-expression was observed [Fig. 3A]. The two genes are structurally highly related, and both genes are present in the human genome, suggesting a gene duplication event prior to the mammalian radiation. Structurally, each gene comprises two exons with a large intronic region. Due to their highly similar sulfotransferase domain and ability to act on the same disaccharide, we expected functional redundancy and therefore generated a double knockout of the two genes. We acquired the *Hs3st3a1*−/− mouse from the trans-NIH Knock-Out Mouse Project (KOMP). Through homologous recombination, a deleted sequence (553bp) directly downstream of the ATG site was replaced with an *E. coli* LacZ gene sequence [Fig. 3B]. This effectively generates LacZ instead of Hs3st3a1 protein during the transcription of this gene. Staining E15.5 Hs3st3a1+/− kidneys for β-galactosidase activity from the lacZ allele demonstrates the ureteric bud tip-specific expression of *Hs3st3a1* [Fig. 3C]. By injecting the appropriate gRNA and Cas9 protein into *Hs3st3a1*−/− fertilized eggs, we generated an 88bp deletion within the first exon of *Hs3st3b1* allele [Fig. 3D]. This deletion includes the predicted ATG site, though a second ATG is encoded 37 amino acids downstream from the deletion. Though this could potentially generate an amino-truncated protein, the protein would lack highly-conserved, amino terminal transmembrane domain sequences. Unfortunately, the absence of antibodies recognizing Hs3st3b1 precludes any additional insight though it may be possible in future studies to develop enzymatic assays to test for residual Hs3st3b1 enzyme activity.

Ureter Duplications in Mutant Kidneys

To determine the viability of the knockout mice generated, heterozygote intercrosses were quantified for percentage of each genotype present per sex and compared to Mendelian frequency. Furthermore, to observe any phenotypes, lung and kidneys were collected at E12.5 for each mutant mouse.

D17H6S56E-5−/− mice generated were adult viable and recovered at close to Mendelian frequency ($x^2 = 5.22$, p = 0.07): 22% (16/74) of pups born from heterozygous intercrosses [Fig. 4A]. Stage-matched heterozygote and knockout lungs were collected at E12.5 and immunostained to visualize cytokeratin (CK, epithelial marker) and vimentin (Vim, mesenchymal marker). The lungs appeared normal [Fig. 4B–D]. E12.5 stage-matched kidneys also showed no obvious difference in the CK-marked ureteric network or adjacent $Six2^+$ nephron progenitor cells though one *D17H6S56E-5*−/− kidney displayed a double ureter (1/28, 3.6%), a frequency not statistically different from spontaneous double ureter formation in the C57BL6/J mouse strain (1/59, 0.02%) [Fig. 4E–G, Fig.5].

The *Tmem59l* knockout mice were adult viable but recovered at a frequency (8/47, 17%) slightly lower but not significantly different from Mendelian expectation in heterozygous intercrosses ($x^2 = 1.60$, p = 0.45) [Fig. 4H]. At E12.5, no branching phenotype was observed in the developing lungs of homozygote lungs [Fig. 4I–K]. A low percentage of kidneys lacking a normal *Tmem59l* gene exhibited a double ureter phenotype (2/23, 8.7%) [Fig. 4L–N]. No phenotype was observed in a similar number of heterozygotes (0/19, 0%) and

comparison with wild-type C57BL6/J kidneys suggests a statistically significant increase in ureter duplication above background levels [*Tmem59l*−/− (x^2 = 6.77, p = 0.0091), Fig.5].

Hs3st3a1/Hs3st3b1 double knockout mice were also adult viable. E12.5 staged-matched lungs did not exhibit any obvious phenotype [Fig. 4O, Q]. On the other hand, embryonic kidneys form double ureters with a low penetrance (3/28, 10.7%), a higher frequency than spontaneous duplications observed in heterozygous compound mutant mice or wildtype C57BL6/J mice [x^2 = 13.67, p = 0.0002; Fig. 4P, R; Fig. 5]. The double ureter formed is not identical in each case, suggesting a variation in the position of ectopic outgrowth from the mesonephric duct, or from the stalk region of the forming ureteric bud.

DISCUSSION

A Shared Double Ureter Phenotype Amongst the UB Tip Knockout Mice

The UB tip progenitor population is a key cell type for the proper development of the collecting duct system and ultimately, the entire organ. Here, we generated four new knockout alleles complementing a recent study on Adamts18[24] which shares with the gene targets in this current study, ureteric and lung branch tip enriched gene expression (excepting Hs3st3b1).[8] Shared expression in the kidney and lung suggested shared programs of gene regulation, and potentially, function. In this light, the mutational outcomes were surprising: no early lung phenotypes where observed in the mutants analyzed here, in contrast to the pronounced growth phenotype reported for *Adamts1*8 mutants, and in the kidney, a weakly penetrant ureter duplication phenotype (excepting *D17H6S56E-5*−/− mice), Relative to SW mice, the C57BL6/J background may be “sensitized” for spontaneous ureter duplication, though certitude would require a more extensive interstrain comparison [Fig. 5] suggesting this background may be particular effective at detecting weak interacting genes, the only phenotype observed in this limited study.

In addition to Adamts18, which encodes a secreted, Adams family metalloprotease, ureter duplications are observed in Robo2 and Slit2 mutants. The high penetrance of these phenotypes enabled the identification of a Robo2/Slit2 driven restriction of GDNF expression as the likely cause of ectopic ureteric bud outgrowths.[25,26] Loss of Wnt5a or Bmp4 results in a wide range of kidney phenotypes including the formation of double ureters; phenotypic analysis suggests these signaling pathways normally act to inhibit and confine UB outgrowth.[27–29] Tmem59l has not been linked to any of these proteins or their known pathways of action. In contrast, Hs3st3a1/Hs3st3b1, modulation of heparin sulfate proteoglycans (HSPGs) could link to both FGF and Wnt signaling where HSPGs play important roles.[30,31]

Congenital Anomaly of Kidney and Urinary Tract (CAKUT) is an extensive and wide-ranging group of abnormalities that occur during kidney and urinary tract development in humans. Some aberrations include renal agenesis, multicystic dysplasic kidneys, double ureters, congenital megaureter, and vesicouretral reflux. CAKUT patients make up about 20–30% of all developmental defects reported and occur in about 1 in every 500 live births.[32,33] Many of the genes that have been identified to be associated with CAKUT are conserved in mice. Moreover, these genes have also been shown to play a role in kidney

development, such as RET, SIX2, and BMP4.[34,35] Currently, none of the genes studied here have been connected to CAKUT in patients.

In summary, while the evidence suggests roles for *Tmem59l* and *Hs3st3a1/Hs3st3b1* in the key initiating step of kidney morphogenesis, ureteric bud outgrowth, the low penetrance of phenotypes seen here presents a significant challenge to obtaining further mechanistic insights into their actions.

EXPERIMENTAL PROCEDURES

Mouse Strains

The Wnt11RFP mouse strain was generated in the McMahon lab (B6;D-Tg(Wnt11-TagRFP/cre/ERT2)28Amc/J; Jackson Laboratory stock 018683).[22] The Hoxb7Venus mouse was generated and provided by Dr. Frank Costantini (Tg(Hoxb7-Venus*)17Cos/J; Jackson Laboratory stock 016252).[23] The *Hs3st3a1*−/− mouse (VG19780) was produced by the trans-NIH Knock-Out Mouse Project (KOMP) and obtained from the KOMP Repository (www.komp.org). Mouse handling, husbandry, and procedures were all performed in compliance with the guidelines established by the Institutional Animal Care and Use Committees (IACUC) at the University of Southern California.

Generation of Knockout Mouse Strains via CRISPR/Cas9 Gene Editing

Standard CRISPR/Cas9 gene editing protocols were used to precisely delete specific regions of the *D17H6S56E-5*, *Hs3st3b1*, and *Tmem59l* genes.[36] Exact details of the mutations are reported in the results. A brief generalized description of the approach follows. PCR-based methods were used to synthesize the DNA templates for Cas9 and sgRNA (single guide RNA). Guide RNA (gRNA) sequences for generating sgRNA DNA templates were identified for each target gene on crispr.mit.edu. Purified PCR products for Cas9 and sgRNAs were mixed with dNTPs and T7 enzyme for *in vitro* transcription. The resulting sgRNA and Cas9 RNA were microinjected into fertilized eggs collected from super ovulating female mice. For *D17H6S56E-5* and *Tmem59l* deletions, injections were performed in C57BL/6J eggs. The *Hs3st3b1* injection was performed in *Hs3st3a1*−/− fertilized eggs. These manipulated zygotes were placed into the oviducts of pseudopregnant foster female mice. Pups were assessed for deleted regions in gene targets by Sanger sequencing of cloned PCR products.

Whole-mount *in situ* Hybridization

In situ hybridization was completed utilizing our previously published procedure.[8] Briefly, tissue samples were collected and fixed overnight in 4% paraformaldehyde (PFA), dehydrated in methanol, and stored at −20°C. Tissue was rehydrated, bleached with 6% hydrogen peroxide, incubated in proteinase K (10 μg/ml), fixed in 4% PFA, pre-hybridized in hybridization buffer at 70°C, and then incubated overnight in a RNA probe that recognized the rtTA sequence. Tissue was transferred to a BioLane HTI machine, which performed formamide washes, antibody incubation, and MBST (100 mM maleic acid, 150 mM NaCl, 0.1% Tween-20) washes. Samples were incubated with BM purple for up to 48hr

to reveal the *in situ* hybridization of the RNA probe, fixed in 4% PFA, and stored in 80% glycerol. Tissue was imaged in an AxioZoom.V16 stereozoom microscope (Zeiss).

Antibody Immunofluorescent Staining

Embryonic lungs and kidneys were harvested and subjected to a short fixation in 4% PFA. For whole-mount staining, tissue was incubated in blocking solution (10% sheep serum, 0.1% Triton, PBS) for 1hr and incubated in primary antibodies at 4°C for 24–48hr. Antibodies used were cytokeratin (1:500; Sigma C2562, Novus Biologicals NB120–11213), Six2 (1:500; Proteintech 11562–1-AP), and vimentin (1:500; Abcam ab92547). Samples were washed in PBST (0.1% Triton, PBS) to remove and residual primary antibody for several hours, and then incubated in the corresponding secondary antibody for 24–48hr at 4°C. Tissue was again washed in PBST for several hours to remove any remaining secondary antibody, and then imaged on an AxioZoom.V16 stereozoom microscope (Zeiss).

For cryosections with native fluorescence in the tissue, embryonic kidneys were harvested, fixed in 4% PFA, incubated overnight in 30% sucrose, embedded in OCT, and stored in −80°C. Cryoblocks were sectioned at 12μm thick (Zeiss Microm HM550 cryostat), placed on glass slides (VWR Superfrost Plus Micro Slide), and stored at −80°C. To remove the OCT, slides were washed in PBS, and then incubated in Hoechst 33342 to stain nuclei. Tissue sections were imaged on a confocal SP8 microscope (Leica) to capture native fluorescent signal.

ACKNOWLEDGEMENTS

We would like to thank Dr. Frank Costantini for graciously providing the Hoxb7Venus mice. The *Hs3st3a1*−/− mouse (VG19780) was generated by the trans-NIH Knock-Out Mouse Project (KOMP) and obtained from the KOMP Repository (www.komp.org). NIH grants to Velocigene at Regeneron Inc (U01HG004085) and the CSD Consortium (U01HG004080) funded the generation of gene-targeted ES cells for 8500 genes in the KOMP Program and archived and distributed by the KOMP Repository at UC Davis and CHORI (U42RR024244). For more information or to obtain KOMP products go to www.komp.org or email service@komp.org.

Grant Sponsor: Work in A.P.M.'s laboratory was funded by a grant from the National Institutes of Health [DK054364]. E.A.R. was supported by a graduate student training fellowship from the National Institutes of Health [5T32HD060549] and by the National Institute of Diabetes and Digestive and Kidney Diseases of the National Institutes of Health [F31DK107216].

REFERENCES

1. Ochoa-Espinosa A, Affolter M. Branching morphogenesis: from cells to organs and back. Cold Spring Harb Perspect Biol 2012;4.
2. Iber D, Menshykau D. The control of branching morphogenesis Open Biol. England, 2013:130088.
3. Costantini F Genetic controls and cellular behaviors in branching morphogenesis of the renal collecting system. Wiley Interdiscip Rev Dev Biol 2012;1:693–713. [PubMed: 22942910]
4. McMahon AP. Development of the Mammalian Kidney. Curr Top Dev Biol 2016;117:31–64. [PubMed: 26969971]
5. Herriges M, Morrisey EE. Lung development: orchestrating the generation and regeneration of a complex organ. Development 2014;141:502–513. [PubMed: 24449833]
6. Rock JR, Hogan BL. Epithelial progenitor cells in lung development, maintenance, repair, and disease. Annu Rev Cell Dev Biol 2011;27:493–512. [PubMed: 21639799]
7. Metzger RJ, Klein OD, Martin GR, Krasnow MA. The branching programme of mouse lung development Nature. England, 2008:745–750.

8. Rutledge EA, Benazet JD, McMahon AP. Cellular heterogeneity in the ureteric progenitor niche and distinct profiles of branching morphogenesis in organ development. Development 2017;144:3177–3188. [PubMed: 28705898]

9. Snoek M, van Dinten L, van Vugt H. A novel gene, G7e, resembling a viral envelope gene, is located at the recombinational hot spot in the class III region of the mouse MHC. Genomics 1996;38:5–12. [PubMed: 8954773]

10. Marcum JA, Atha DH, Fritze LM, Nawroth P, Stern D, Rosenberg RD. Cloned bovine aortic endothelial cells synthesize anticoagulantly active heparan sulfate proteoglycan. J Biol Chem 1986;261:7507–7517. [PubMed: 2940242]

11. Pejler G, Danielsson A, Bjork I, Lindahl U, Nader HB, Dietrich CP. Structure and antithrombin-binding properties of heparin isolated from the clams Anomalocardia brasiliana and Tivela mactroides. J Biol Chem 1987;262:11413–11421. [PubMed: 3624220]

12. Zhang L, Lawrence R, Schwartz JJ, Bai X, Wei G, Esko JD, Rosenberg RD. The effect of precursor structures on the action of glucosaminyl 3-O-sulfotransferase-1 and the biosynthesis of anticoagulant heparan sulfate. J Biol Chem 2001;276:28806–28813. [PubMed: 11375390]

13. de Agostini AI, Dong JC, de Vantery Arrighi C, Ramus MA, Dentand-Quadri I, Thalmann S, Ventura P, Ibecheole V, Monge F, Fischer AM, HajMohammadi S, Shworak NW, Zhang L, Zhang Z, Linhardt RJ. Human follicular fluid heparan sulfate contains abundant 3-O-sulfated chains with anticoagulant activity. J Biol Chem 2008;283:28115–28124. [PubMed: 18669628]

14. Shworak NW, Liu J, Petros LM, Zhang L, Kobayashi M, Copeland NG, Jenkins NA, Rosenberg RD. Multiple isoforms of heparan sulfate D-glucosaminyl 3-O-sulfotransferase. Isolation, characterization, and expression of human cdnas and identification of distinct genomic loci. J Biol Chem 1999;274:5170–5184. [PubMed: 9988767]

15. Mohammadi M, Olsen SK, Ibrahimi OA. Structural basis for fibroblast growth factor receptor activation. Cytokine Growth Factor Rev 2005;16:107–137. [PubMed: 15863029]

16. Patel VN, Lombaert IM, Cowherd SN, Shworak NW, Xu Y, Liu J, Hoffman MP. Hs3st3-modified heparan sulfate controls KIT+ progenitor expansion by regulating 3-O-sulfotransferases. Dev Cell 2014;29:662–673. [PubMed: 24960693]

17. Barnett MW, Fisher CE, Perona-Wright G, Davies JA. Signalling by glial cell line-derived neurotrophic factor (GDNF) requires heparan sulphate glycosaminoglycan. J Cell Sci 2002;115:4495–4503. [PubMed: 12414995]

18. Davies JA, Yates EA, Turnbull JE. Structural determinants of heparan sulphate modulation of GDNF signalling. Growth Factors 2003;21:109–119. [PubMed: 14708939]

19. Elson GC, de Coignac AB, Aubry JP, Delneste Y, Magistrelli G, Holzwarth J, Bonnefoy JY, Gauchat JF. BSMAP, a novel protein expressed specifically in the brain whose gene is localized on chromosome 19p12. Biochem Biophys Res Commun 1999;264:55–62. [PubMed: 10527841]

20. Ullrich S, Munch A, Neumann S, Kremmer E, Tatzelt J, Lichtenthaler SF. The novel membrane protein TMEM59 modulates complex glycosylation, cell surface expression, and secretion of the amyloid precursor protein. J Biol Chem 2010;285:20664–20674. [PubMed: 20427278]

21. Zheng Q, Zheng X, Zhang L, Luo H, Qian L, Fu X, Liu Y, Gao Y, Niu M, Meng J, Zhang M, Bu G, Xu H, Zhang YW. The Neuron-Specific Protein TMEM59L Mediates Oxidative Stress-Induced Cell Death. Mol Neurobiol 2017;54:4189–4200. [PubMed: 27324899]

22. Harding SD, Armit C, Armstrong J, Brennan J, Cheng Y, Haggarty B, Houghton D, Lloyd-MacGilp S, Pi X, Roochun Y, Sharghi M, Tindal C, McMahon AP, Gottesman B, Little MH, Georgas K, Aronow BJ, Potter SS, Brunskill EW, Southard-Smith EM, Mendelsohn C, Baldock RA, Davies JA, Davidson D. The GUDMAP database--an online resource for genitourinary research. Development 2011;138:2845–2853. [PubMed: 21652655]

23. Chi X, Hadjantonakis AK, Wu Z, Hyink D, Costantini F. A transgenic mouse that reveals cell shape and arrangement during ureteric bud branching. Genesis 2009;47:61–66. [PubMed: 19111008]

24. Rutledge EA, Parvez RK, Short KM, Smyth IM, McMahon AP. Morphogenesis of the kidney and lung requires branch-tip directed activity of the Adamts18 metalloprotease. Dev Biol 2019;454:156–169. [PubMed: 31242448]

25. Grieshammer U, Le M, Plump AS, Wang F, Tessier-Lavigne M, Martin GR. SLIT2-mediated ROBO2 signaling restricts kidney induction to a single site. Dev Cell 2004;6:709–717. [PubMed: 15130495]

26. Wainwright EN, Wilhelm D, Combes AN, Little MH, Koopman P. ROBO2 restricts the nephrogenic field and regulates Wolffian duct-nephrogenic cord separation. Dev Biol 2015;404:88–102. [PubMed: 26116176]

27. Pietila I, Prunskaite-Hyyrylainen R, Kaisto S, Tika E, van Eerde AM, Salo AM, Garma L, Miinalainen I, Feitz WF, Bongers EM, Juffer A, Knoers NV, Renkema KY, Myllyharju J, Vainio SJ. Wnt5a Deficiency Leads to Anomalies in Ureteric Tree Development, Tubular Epithelial Cell Organization and Basement Membrane Integrity Pointing to a Role in Kidney Collecting Duct Patterning. PLoS One 2016;11:e0147171. [PubMed: 26794322]

28. Miyazaki Y, Oshima K, Fogo A, Hogan BL, Ichikawa I. Bone morphogenetic protein 4 regulates the budding site and elongation of the mouse ureter. J Clin Invest 2000;105:863–873. [PubMed: 10749566]

29. Dudley AT, Robertson EJ. Overlapping expression domains of bone morphogenetic protein family members potentially account for limited tissue defects in BMP7 deficient embryos. Dev Dyn 1997;208:349–362. [PubMed: 9056639]

30. Nakato H, Li JP. Functions of Heparan Sulfate Proteoglycans in Development: Insights From Drosophila Models. Int Rev Cell Mol Biol 2016;325:275–293. [PubMed: 27241223]

31. Poulain FE, Yost HJ. Heparan sulfate proteoglycans: a sugar code for vertebrate development? Development 2015;142:3456–3467. [PubMed: 26487777]

32. Song R, Yosypiv IV. Genetics of congenital anomalies of the kidney and urinary tract. Pediatr Nephrol 2011;26:353–364. [PubMed: 20798957]

33. Uy N, Reidy K. Developmental Genetics and Congenital Anomalies of the Kidney and Urinary Tract. J Pediatr Genet 2016;5:51–60. [PubMed: 27617142]

34. Hildebrandt F Genetic kidney diseases. Lancet 2010;375:1287–1295. [PubMed: 20382325]

35. Nicolaou N, Renkema KY, Bongers EM, Giles RH, Knoers NV. Genetic, environmental, and epigenetic factors involved in CAKUT. Nat Rev Nephrol 2015;11:720–731. [PubMed: 26281895]

36. Harms DW, Quadros RM, Seruggia D, Ohtsuka M, Takahashi G, Montoliu L, Gurumurthy CB. Mouse Genome Editing Using the CRISPR/Cas System. Curr Protoc Hum Genet 2014;83:15.17.11–27. [PubMed: 25271839]

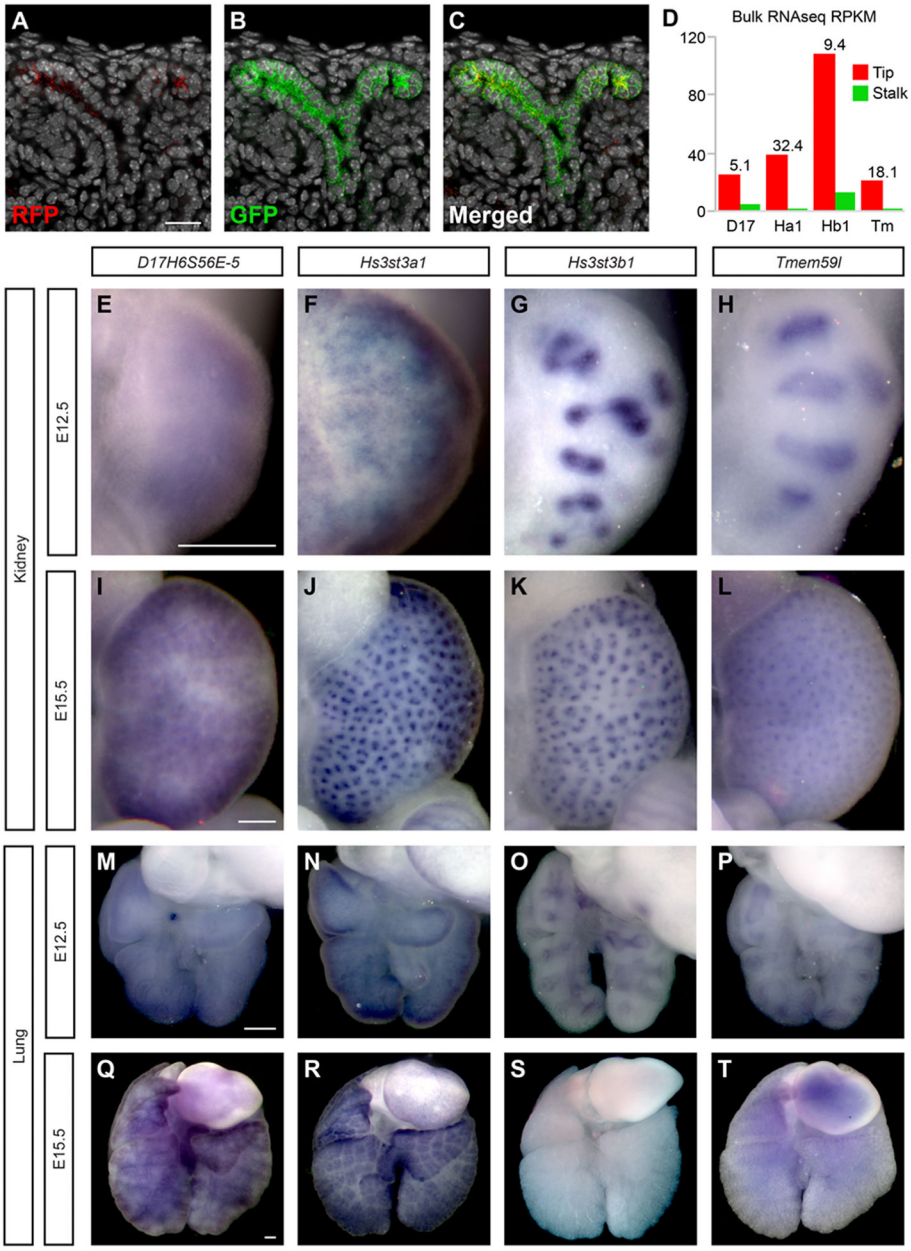

Fig. 1: Identification of four ureteric bud tip genes through an embryonic kidney bulk RNA sequencing screen.

A-C: Cryosection of a E16.5 kidney from a Hoxb7Venus;Wnt11RFP mouse showcasing ureteric epithelium (GFP) and the tip population (RFP) collected via dissociation and FACs for the bulk RNA sequencing screen comparing tip vs stalk. **D:** Fold change (FC) and reads per kilobase per million (RPKM) values of four genes of interest from the RNA sequencing screen. **E-T:** Whole-mount *in situ* hybridization staining of at E12.5 and E15.5 embryonic kidneys (E-L) and lungs (M-T) of the four genes of interest. Line in A = 20μm; Line in E, I, M, Q = 200μm.

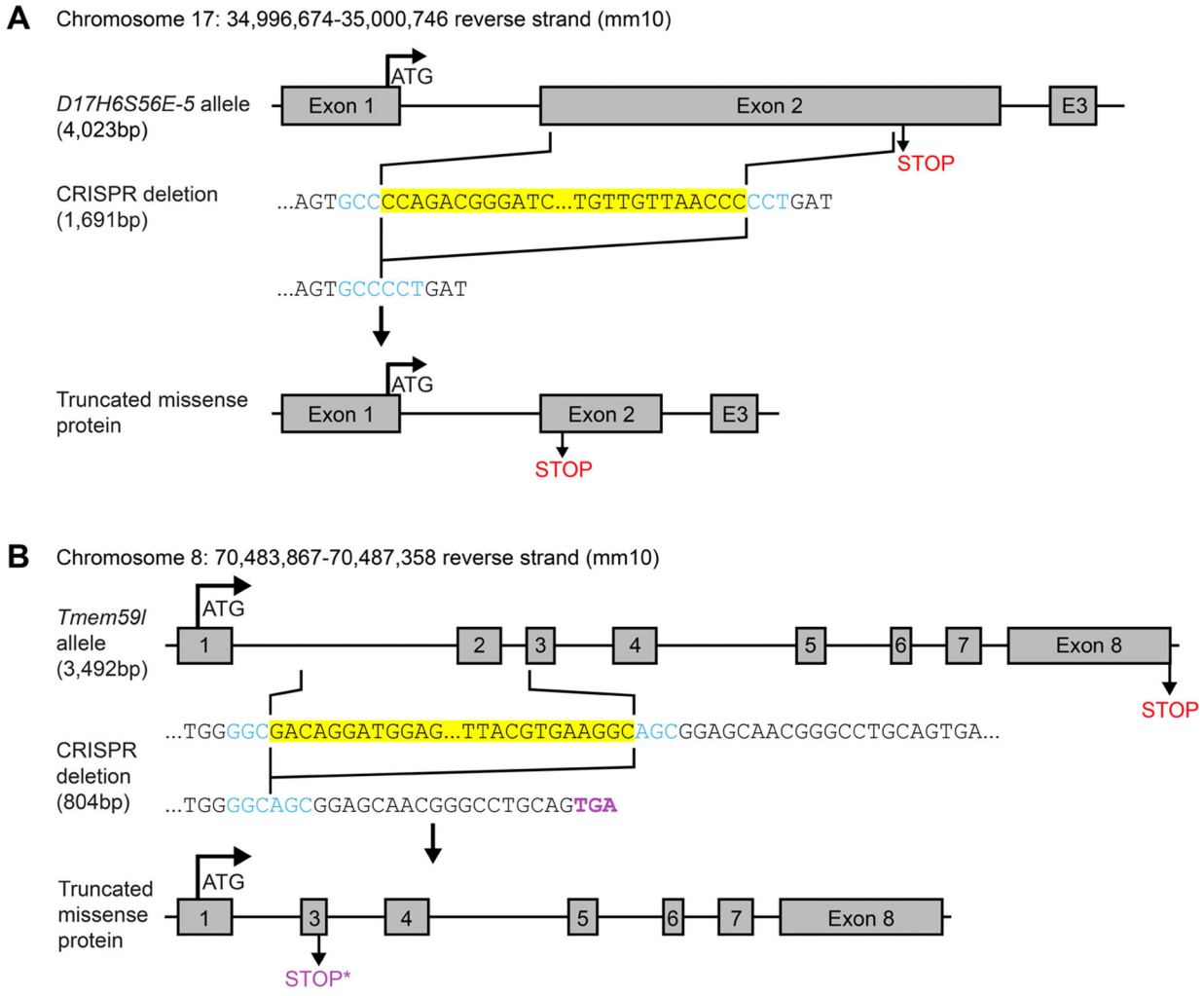

Fig. 2: CRISPR/Cas9 gene editing at specific loci resulted in the generation of knockout mice.

A: Wildtype allele of *D17H6S56E-5* gene and the CRISPR/Cas9 deletion (highlighted in yellow) that leads to the generation of a truncated missense protein in the *D17H6S56E-5*−/− mouse model. **B:** CRISPR/Cas9 deletion (highlighted in yellow) downstream of ATG site leads to the creation of a new STOP codon (labeled with an asterisk) and the generation of a truncated missense protein.

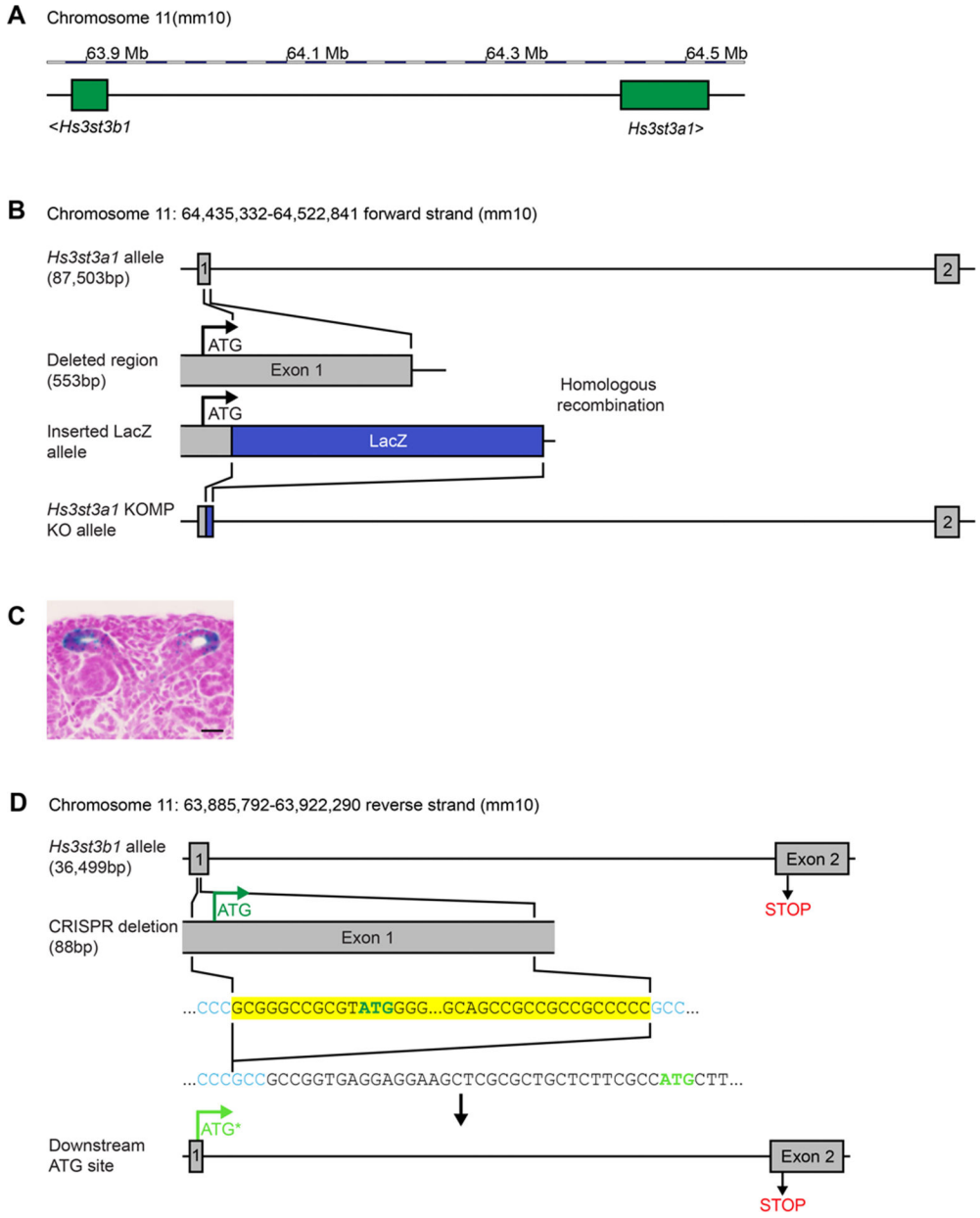

Fig 3: Gene editing via CRISPR/Cas9 on the *Hs3st3a1*−/− mouse resulted in the generation of the *Hs3st3a1*−/−;*Hs3st3b1*−/− mouse.

A: The *Hs3st3a1* gene is located 511bp downstream from *Hs3st3b1* on chromosome 11 **B:** The *Hs3st3a1*−/− mouse was generated through the NIH-funded Knock Out Mouse Project, A region directly downstream of the ATG site was deleted and replaced by an *E. coli* LacZ casette. **C:** LacZ staining on E15.5 *Hs3st3a1*+/− kidney demonstrating ureteric bud tip expression **D:** The *Hs3st3b1*−/− knockout was produced through a CRISPR/Cas9 deletion that included the ATG site in Exon 1 (highlighted in yellow). A second in-frame ATG site is located downstream in Exon 1, demarcated with the asterisk, which may enable initiation of a truncated protein. Line = 20μm.

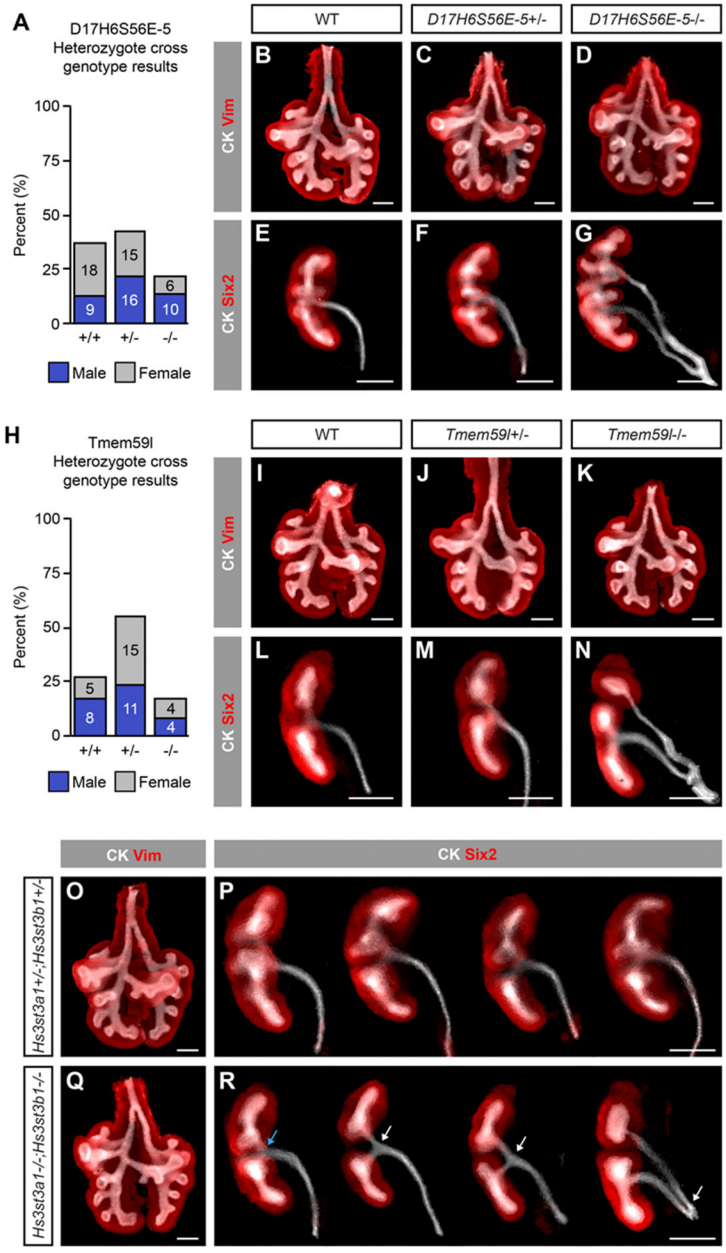

Fig. 4: Knockout mice at E12.5 demonstrate double ureter kidneys at low frequencies with no lung phenotype.

A: *D17H6S56E-5* heterozygous intercross results show similar Mendelian frequency to expected (numbers on bar graph are the number of each sex per genotype, $x^2 = 5.22$, p = 0.07). **B-G:** *D17H6S56E-5* lungs (B-D) and kidneys (E-G) stained with cytokeratin (CK, epithelial marker), vimentin (Vim, lung mesenchyme marker), and Six2 (kidney nephron progenitor marker). *D17H6S56E-5*−/− kidneys display a double ureter phenotype in 3.6% (G). **H:** Percentage of wildtype, heterozygote, and knockout pups born from *Tmem59l*+/− parents follow expected Mendelian frequency ($x^2 = 1.60$, p = 0.45). **I-K:** *Tmem59l* lungs stained with CK and Vim. **L-N:** *Tmem59l* kidneys stained with CK and Six2. The loss of *Tmem59l* results in the presence of a double ureter at 8.7% frequency. **O-R**: *Hs3st3a1*+/

−;*Hs3st3b1*+/− and *Hs3st3a1*−/−;*Hs3st3b1*−/− lungs (O, Q) and kidneys (P, R) stained with CK and either Vim (lung) or Six2 (kidneys). There is no observed phenotype in the lungs, whereas a 10.7% of *Hs3st3a1*−/−;*Hs3st3b1*−/− kidneys display a double ureter phenotype. Blue arrow: first branching event within the Six2+ population. White arrow: first branching event outside of Six2+ population in double ureter kidneys. Line = 200μm.

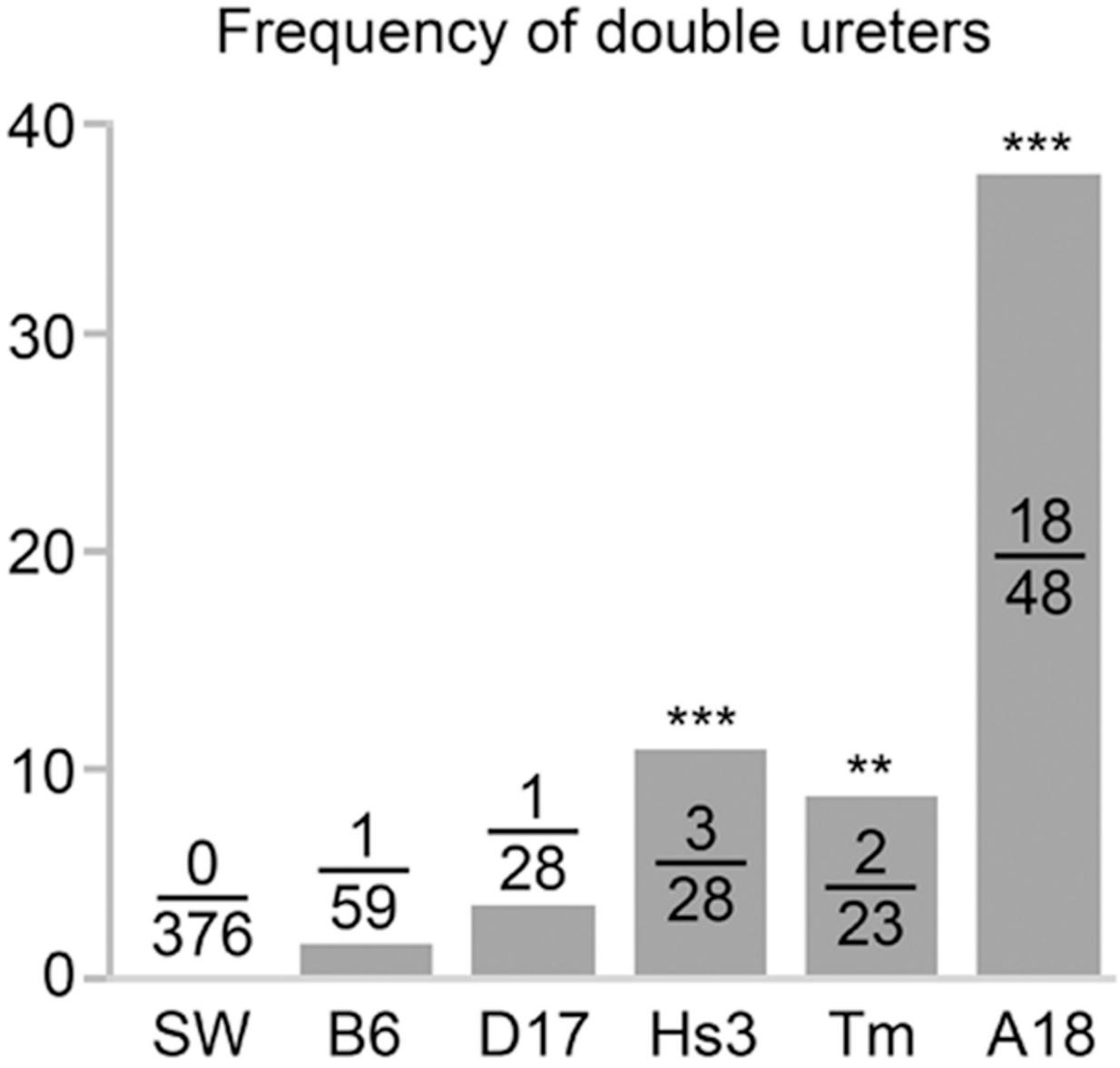

Fig. 5: Frequencies of double ureters across mouse lines.

Swiss Webster (SW) mice have a very low frequency of double ureter formation, none were detected examining 376 E12.5 kidneys. In contrast, C57BL6/J (B6) mice showed a low, spontaneous frequency of unilateral double ureter formation. We have reported[8,24] mutants in Adamts18, a metalloprotease identified in the same UPC-targeted expression screen, display a marked increase in ureter duplications (x^2 = 369.32, p < 0.0001). *Hs3st3a1*−/−;*Hs3st3b1*−/− (x^2 = 13.67, p = 0.0002) and *Tmem59l*−/− (x^2 = 6.77, p = 0.0091) mutant kidneys showed a significantly higher double ureter frequencies than B6 controls. ** = p < 0.01, *** = p < 0.001.